Y. Bai, J.D. Biggs, F. Bernelli Zazzera, N. Cui
*Adaptive Attitude Tracking with Active Uncertainty Rejection*
Journal of Guidance Control and Dynamics, Vol. 41, N. 2, 2018, p. 546-554
doi:10.2514/1.G002391

# Adaptive attitude tracking with active uncertainty rejection

Yuliang Bai*, James D. Biggs†, Franco Bernelli Zazzera‡, Naigang Cui§

*Harbin Institute of Technology, Harbin, 150001, China.*,

*Politecnico di Milano, Milano, 20156, Italy.*,

*Politecnico di Milano, Milano, 20156, Italy.*,

*Harbin Institute of Technology, Harbin, 150001, China.*

## Nomenclature

| | | |
|---|---|---|
| $\bar{\boldsymbol{q}}$,$\boldsymbol{q}$,$q_4$ | = | quaternion of spacecraft |
| $\bar{\boldsymbol{q}}_d$,$\boldsymbol{q}_d$,$q_{d4}$ | = | desired quaternion of spacecraft |
| $\bar{\boldsymbol{q}}_e$,$\boldsymbol{q}_e$,$q_{e4}$ | = | error quaternion of spacecraft |
| $J$ | = | inertia matrix of spacecraft |
| $\boldsymbol{\omega}$ | = | angular velocity vector of spacecraft, $rad/s$ |
| $\boldsymbol{\omega}_d$ | = | target angular velocity vector of spacecraft, $rad/s$ |
| $\boldsymbol{\omega}_e$ | = | error angular velocity vector of spacecraft, $rad/s$ |
| $\boldsymbol{\Omega}$ | = | angular velocity vector of reaction wheels, $rad/s$ |
| $\boldsymbol{C}$ | = | direction cosine matrix from the inertial frame to the body frame |
| $\boldsymbol{u}$ | = | control torque, $N \cdot m$ |
| $\boldsymbol{d}$ | = | external disturbance torques, $N \cdot m$ |
| $\boldsymbol{d}_f$ | = | friction of reaction wheels, $N \cdot m$ |
| $\boldsymbol{f}$ | = | total uncertainties |

*Research Assistant, School of Astronautics, Mailbox 345, Heilongjiang.
†Associate Professor, Department of Aerospace Science & Technology.
‡Professor, Department of Aerospace Science & Technology.
§Professor, School of Astronautics, Mailbox 345, Heilongjiang.

# I. Introduction

Challenging future space missions to asteroids and planets are complicated by uncertainty in disturbances such as gravitational fields, drag and solar radiation pressure. Furthermore, uncertainties in reaction wheel (RW) friction and the moments of inertia of a spacecraft, due to sloshing and flexible parts, can lead to inefficient attitude control design. For the success of some future missions it will be necessary to develop attitude control algorithms that can efficiently slew or track a prescribed trajectory in the presence of such uncertainties. This paper develops an adaptive linear uncertainty rejection control for attitude tracking based on the fusion of an adaptive quaternion feedback control and a linear extended state observer (LESO). The proposed method estimates the uncertain moments of inertia, environmental disturbance torques and RW friction and compensates for them in each sampling period to ensure that the attitude converges to a small neighborhood of the desired motion. It is shown that, after an initial transient, an upper-limit on the tracking error can be analytically defined in terms of the control gains. Both the adaptive law and LESO are simple to implement and tune. The control is tested in simulation on a 3U CubeSat and is shown to efficiently re-point it in the presence of uncertainties and improve the pointing accuracy when compared to a proportional derivative tracking controller for our chosen examples. As an additional practical example the control is shown to effectively stabilize a nano-spacecraft in the presence of significant RW friction.

The attitude control of spacecraft in the presence of disturbances and uncertain modeling parameters has been extensively studied. Several different approaches include robust control [1,2], adaptive control [1–7] and sliding mode control [8–10]. Generally, robust control methods can achieve bounded disturbance rejection. However, it requires knowledge of the bound of the disturbance and cancels it in the control [11,12] which can lead to an excessive use of torque. Adaptive control methods can ensure tracking accuracy by adapting the gains using simple deterministic or fuzzy rules, but require knowledge of the parametric uncertainty or disturbances such as the upper bound and frequency. Sliding mode control has been shown to provide robustness to disturbances, but can lead to chattering; a significant problem which can excite the flexible modes of spacecraft appendages. In [13], the authors demonstrate the efficient control of a spacecraft where a finite

sum of sinusoidal functions is used to represent periodic disturbances without knowledge of the amplitude and phase angles, but does require knowledge of their frequency.

Active disturbance rejection control (ADRC) has been demonstrated to effectively control systems in the presence of external disturbance uncertainties and does not require any information of them [14–16]. Moreover, the ADRC method estimates the bounds of the disturbances using an extended state observer (ESO) and compensates for them at each sampling period. The ADRC method combined with a sliding-mode controller [17] was used to develop an attitude control method that is robust to parametric uncertainties and disturbances. The ADRC method has also been combined with a simple quaternion PID control that uses fuzzy logic to choose the gains to stabilize a spacecraft in the presence of uncertainty [18]. However, the stability of this control [18] is not proved analytically and it does not address the tracking problem. Adaptive attitude controls have been demonstrated in [19] to deal with unknown disturbances. However, the control law [19] has a singularity in the differential equation that defines the adaptive parameter and it requires a saturation function to be defined in order to avoid this singularity. In addition, the stability proof in [19] relies on the strong assumption of a perfect estimation of disturbances. In this note, an adaptive attitude tracking control with active uncertainty rejection and a continuous adaptive parameter is developed that guarantees asymptotic convergence to a small bounded region of the desired trajectory even in the presence of estimation errors.

In this note we combine an adaptive variation of the flight-tested quaternion feedback control [7] with a linear extended state observer (LESO) [20] to develop an analytically verifiable and robust tracking control that avoids any potential complications that can be caused by chattering. LESO is employed rather than a nonlinear observer as it is easy to tune, in particular, it requires the tuning of only two parameters in contrast to choosing four parameters of the nonlinear extended state observer [21]. The controlled motion of the spacecraft is shown to converge to a neighborhood of the desired motion in the presence of uncertainties in both modeling parameters and disturbances torques. Furthermore, the inclusion of the adaptive parameter enables the upper-bound on the tracking error to be controlled via the control gains. However, in practise the gains will be constrained by the maximum available torque of the actuator. As an additional example it is

demonstrated that the control can increase the pointing accuracy of a spacecraft relative to a typical proportional controller in the presence of significant RW friction. Previously attitude tracking of spacecraft with unknown RW friction has been addressed using a quaternion feedback controller with adaptive gains that follow simple deterministic rules. In this case the control law requires apriori knowledge of the bounds on the reaction wheel friction.

In Section II, the attitude kinematics and dynamics of the spacecraft in the presence of uncertainties are formulated in a convenient form for the application of LESO. Section III addresses the problem of developing an adaptive linear disturbance rejection control (ALDRC) in the presence of uncertainties in the inertia matrix and external torques. For the proposed control law, we construct a suitable Lyapunov function to prove that the spacecraft tracks the desired trajectory within a small neighborhood of the desired motion. In Section IV, simulations are undertaken using the model of a 3U CubeSat which illustrates the robustness of the proposed control method to unknown disturbances, parametric uncertainty and unpredictable RW friction and provides a significant improvement, for the chosen example, over strictly adaptive quaternion laws [7,22].

## II. Attitude dynamics and kinematics of a rigid-spacecraft

The spacecraft is assumed to be a rigid body described by the dynamics and kinematics [23]:

$$J\dot{\boldsymbol{\omega}} = -\boldsymbol{\omega}^{\times} J\boldsymbol{\omega} + \boldsymbol{u} + \boldsymbol{d} \tag{1}$$

$$\begin{aligned} \dot{\boldsymbol{q}} &= \tfrac{1}{2}\left(q_4\boldsymbol{\omega} - \boldsymbol{\omega}^{\times}\boldsymbol{q}\right) \\ \dot{q}_4 &= -\tfrac{1}{2}\boldsymbol{\omega}^T\boldsymbol{q} \end{aligned} \tag{2}$$

where, $J \in \mathbb{R}^{3\times3}$ is the positive definite and symmetric inertia tensor, $\boldsymbol{\omega}$=$[\omega_1, \omega_2, \omega_3]^T$ indicates the angular velocity vector with respect to the inertial frame and expressed in body coordinates, $\boldsymbol{u} = [u_1, u_2, u_3]^T$ the control torque and $\boldsymbol{d}$ is the unknown external disturbance, the unit quaternion is $\bar{\boldsymbol{q}} = [q_1, q_2, q_3, q_4]^T$, which can be expressed equivalently as $\bar{\boldsymbol{q}} = \left[\boldsymbol{q}^T, q_4\right]^T$ with $\boldsymbol{q} = [q_1, q_2, q_3]^T$

and such that $\boldsymbol{q}^T\boldsymbol{q} + q_4^2 = 1$, the $^\times$ denotes an operator, such that

$$\boldsymbol{\omega}^\times = \begin{bmatrix} 0 & -\omega_3 & \omega_2 \\ \omega_3 & 0 & -\omega_1 \\ -\omega_2 & \omega_1 & 0 \end{bmatrix}$$

It is assumed that unit quaternion $\bar{\boldsymbol{q}}$ and angular velocity $\boldsymbol{\omega}$ of spacecraft in Eq.(1) and Eq.(2) are measured perfectly. The parametric uncertainty in the moments of inertia can be expressed as:

$$J = J_0 + \Delta J \tag{3}$$

where, $J_0$ is the assumed positive definite nominal inertia matrix and $\Delta J$ indicates the uncertain error and thus Eq.(1) can be expressed as

$$J_0\dot{\boldsymbol{\omega}} = -\boldsymbol{\omega}^\times J_0\boldsymbol{\omega} - \boldsymbol{\omega}^\times\Delta J\boldsymbol{\omega} - \Delta J\dot{\boldsymbol{\omega}} + \boldsymbol{u} + \boldsymbol{d}. \tag{4}$$

The attitude control objective is to track a desired time-dependent quaternion $\bar{\boldsymbol{q}}_d(t)$ and angular velocity $\boldsymbol{\omega}_d(t)$ which satisfies the kinematic equation

$$\begin{aligned} \dot{\boldsymbol{q}}_d &= \tfrac{1}{2}\left(q_{d4}\boldsymbol{\omega}_d - \boldsymbol{\omega}_d^\times\boldsymbol{q}_d\right) \\ \dot{q}_{d4} &= -\tfrac{1}{2}\boldsymbol{\omega}_d^T\boldsymbol{q}_d \end{aligned} \tag{5}$$

where $\bar{\boldsymbol{q}}_d = \left[\boldsymbol{q}_d^T, q_{d4}\right]^T$ with $\boldsymbol{q}_d = [q_{d1}, q_{d2}, q_{d3}]^T$ and $\boldsymbol{q}_d^T\boldsymbol{q}_d + q_{d4}^2 = 1$ denotes the desired attitude quaternion and $\boldsymbol{\omega}_d$ the target angular velocity.

The error quaternion $\bar{\boldsymbol{q}}_e = \left[\boldsymbol{q}_e^T, q_{e4}\right]^T$ where $\boldsymbol{q}_e = [q_{e1}, q_{e2}, q_{e3}]^T$ is defined as $\bar{\boldsymbol{q}}_e = \bar{\boldsymbol{q}}_d^{-1} \otimes \bar{\boldsymbol{q}}$, where $\otimes$ denotes quaternion multiplication. The error kinematics are then expressed as [23]

$$\begin{aligned} \dot{\boldsymbol{q}}_e &= \tfrac{1}{2}\left(q_{e4}\boldsymbol{\omega}_e - \boldsymbol{\omega}_e^\times\boldsymbol{q}_e\right) \\ \dot{q}_{e4} &= -\tfrac{1}{2}\boldsymbol{\omega}_e^T\boldsymbol{q}_e \end{aligned} \tag{6}$$

where $\boldsymbol{q}_e$ and $q_{e4}$ satisfying $\boldsymbol{q}_e^T\boldsymbol{q}_e + q_{e4}^2 = 1$ denotes the error attitude quaternion and $\boldsymbol{\omega}_e = \boldsymbol{\omega} - \boldsymbol{C}\boldsymbol{\omega}_d$

is the error angular velocity with $\boldsymbol{C} = \left(q_{e4}^2 - \boldsymbol{q}_e^T \boldsymbol{q}_e\right) I_3 + 2\boldsymbol{q}_e \boldsymbol{q}_e^T - 2q_{e4}\boldsymbol{q}_e^\times$ [24]. The error dynamics can be expressed as:

$$\dot{\boldsymbol{\omega}}_e = \boldsymbol{F} + \boldsymbol{f} + J_0^{-1}\boldsymbol{u} \tag{7}$$

where $\boldsymbol{f} = \boldsymbol{G} + J_0^{-1}\boldsymbol{d}$ with

$$\begin{aligned} \boldsymbol{G} &= -J_0^{-1}(\boldsymbol{\omega}_e + \boldsymbol{C}\boldsymbol{\omega}_d)^\times \Delta J\,(\boldsymbol{\omega}_e + \boldsymbol{C}\boldsymbol{\omega}_d) - J_0^{-1}\Delta J\,(\dot{\boldsymbol{\omega}}_e - \boldsymbol{\omega}_e^\times \boldsymbol{C}\boldsymbol{\omega}_d + \boldsymbol{C}\dot{\boldsymbol{\omega}}_d) \\ \boldsymbol{F} &= -J_0^{-1}(\boldsymbol{\omega}_e + \boldsymbol{C}\boldsymbol{\omega}_d)^\times J_0\,(\boldsymbol{\omega}_e + \boldsymbol{C}\boldsymbol{\omega}_d) + \boldsymbol{\omega}_e^\times \boldsymbol{C}\boldsymbol{\omega}_d - \boldsymbol{C}\dot{\boldsymbol{\omega}}_d. \end{aligned} \tag{8}$$

Here $\boldsymbol{F}$ is assumed to be known ($\bar{\boldsymbol{q}}$, $\boldsymbol{\omega}$, for example, can be measured by a star tracker and gyroscope respectively and then $\boldsymbol{F}$ computed) and the uncertain disturbance $\boldsymbol{f}$ is estimated by LESO. Assuming $\boldsymbol{f}$ is at least class $C^1$ piecewise differentiable on an interval $t \in [t_0, t_1]$ such $\boldsymbol{\chi} = \dot{\boldsymbol{f}}$ then (7) can be expressed in the form

$$\begin{aligned} \dot{\boldsymbol{\omega}}_e &= \boldsymbol{f} + \boldsymbol{F} + J_0^{-1}\boldsymbol{u} \\ \dot{\boldsymbol{f}} &= \boldsymbol{\chi} \end{aligned} \tag{9}$$

where $\boldsymbol{\omega}_e = [\omega_{e1}, \omega_{e2}, \omega_{e3}]^T$ and $\boldsymbol{f} = [f_1, f_2, f_3]^T$ defines an linear extended state observer on $t \in [t_0, t_1]$. Note that because the disturbance must be differentiable of class $C^1$ that the control cannot include the general case of disturbances with white noise.

## III. Adaptive Disturbance Rejection Attitude Control Strategy

In this section, the adaptive disturbance rejection control strategy is presented where the external disturbances and parametric uncertainties $\boldsymbol{f}$ are estimated by LESO and compensated for at each sampling period to ensure convergence to a neighborhood of the desired attitude.

### A. LESO Design and Convergence Proof

In [21], a general nonlinear state observer is presented that can accurately measure disturbances in nonlinear systems of ordinary differential equations. It is shown that a special case of the nonlinear state observer is linear which is much simpler to tune. In this note the linear estimator is used because it's simple to tune and is less computationally intensive. To estimate the total

disturbance $\boldsymbol{f}$ we use a linear second-order extended state observer [20]

$$\begin{aligned}\dot{\hat{\boldsymbol{\omega}}}_e &= \hat{\boldsymbol{f}} + \beta_1 (\boldsymbol{\omega}_e - \hat{\boldsymbol{\omega}}_e) + \boldsymbol{F} + J_0^{-1}\boldsymbol{u} \\ \dot{\hat{\boldsymbol{f}}} &= \beta_2 (\boldsymbol{\omega}_e - \hat{\boldsymbol{\omega}}_e)\end{aligned} \tag{10}$$

where $\hat{\boldsymbol{\omega}}_e = [\hat{\omega}_{e1}, \hat{\omega}_{e2}, \hat{\omega}_{e3}]^T$ is the estimated value of $\boldsymbol{\omega}_e$ and $\hat{\boldsymbol{f}} = \left[\hat{f}_1, \hat{f}_2, \hat{f}_3\right]^T$ is the estimated value of $\boldsymbol{f}$. The parameters $\beta_1$ and $\beta_2$ are the LESO gains which are defined in terms of the bandwidth $w_c > 0$ as $\beta_1 = 3w_c$ and $\beta_2 = 2w_c^2$. Then defining the estimated error as $\tilde{\boldsymbol{\omega}}_e = \boldsymbol{\omega}_e - \hat{\boldsymbol{\omega}}_e$ and $\tilde{\boldsymbol{f}} = \boldsymbol{f} - \hat{\boldsymbol{f}}$ with $\boldsymbol{\omega}_e$, $\boldsymbol{f}$ defined by Eq.(9) and $\hat{\boldsymbol{\omega}}_e$, $\hat{\boldsymbol{f}}$ defined by Eq.(10), then the estimation error dynamics are

$$\begin{aligned}\dot{\tilde{\boldsymbol{\omega}}}_e &= -3w_c\tilde{\boldsymbol{\omega}}_e + \tilde{\boldsymbol{f}} \\ \dot{\tilde{\boldsymbol{f}}} &= -2w_c^2\tilde{\boldsymbol{\omega}}_e + \boldsymbol{\chi}\end{aligned} \tag{11}$$

To show this we set $\boldsymbol{\varepsilon} = [\boldsymbol{\varepsilon}_1, \boldsymbol{\varepsilon}_2]^T$ and $\boldsymbol{\varepsilon}_1 = \tilde{\boldsymbol{\omega}}_e$, $\boldsymbol{\varepsilon}_2 = \frac{\tilde{f}}{w_c}$, then Eq.(11) becomes

$$\begin{cases}\dot{\boldsymbol{\varepsilon}}_1 = w_c\boldsymbol{\varepsilon}_2 - 3w_c\boldsymbol{\varepsilon}_1 \\ \dot{\boldsymbol{\varepsilon}}_2 = -2w_c\boldsymbol{\varepsilon}_1 + \boldsymbol{\chi}/w_c\end{cases} \Rightarrow \dot{\boldsymbol{\varepsilon}} = w_c A\boldsymbol{\varepsilon} + B\frac{\boldsymbol{\chi}}{w_c} \tag{12}$$

where $\boldsymbol{\varepsilon}_1 = [\varepsilon_{11}, \varepsilon_{12}, \varepsilon_{13}]^T$, $\boldsymbol{\varepsilon}_2 = [\varepsilon_{21}, \varepsilon_{22}, \varepsilon_{23}]^T$, $\boldsymbol{\chi} = [\chi_1, \chi_2, \chi_3]^T$, $A = \begin{bmatrix} -3I_3 & I_3 \\ -2I_3 & \mathbf{0} \end{bmatrix}$ and $B = \begin{bmatrix} \mathbf{0} \\ I_3 \end{bmatrix}$.

Defining the new variables $\tilde{\boldsymbol{\varepsilon}}_1 = [\varepsilon_{11}, \varepsilon_{21}]^T$, $\tilde{\boldsymbol{\varepsilon}}_2 = [\varepsilon_{12}, \varepsilon_{22}]^T$ and $\tilde{\boldsymbol{\varepsilon}}_3 = [\varepsilon_{13}, \varepsilon_{23}]^T$. Then the Eq.(12) will be become as

$$\dot{\tilde{\boldsymbol{\varepsilon}}}_i = \tilde{A}\tilde{\boldsymbol{\varepsilon}}_i + \tilde{B}\frac{\chi_i}{w_c} \tag{13}$$

where $\tilde{A} = \begin{bmatrix} -3w_c & w_c \\ -2w_c & 0 \end{bmatrix}$ and $\tilde{B} = \begin{bmatrix} 0 \\ 1 \end{bmatrix}$.

The solution to Eq.(13) is of the form

$$\tilde{\boldsymbol{\varepsilon}}_i(t) = \exp\left(\tilde{A}t\right)\tilde{\boldsymbol{\varepsilon}}_i(0) + \int_0^t \exp\left[\tilde{A}(t-\tau)\right]\frac{\tilde{B}\chi_i}{w_c}d\tau \tag{14}$$

Using the Cayley-Hamilton theorem we have $\exp(\tilde{A}t)$ as following

$$\exp(\tilde{A}t) = \begin{bmatrix} 2e^{-2w_c t} - e^{-w_c t} & e^{-w_c t} - e^{-2w_c t} \\ 2e^{-2w_c t} - 2e^{-w_c t} & 2e^{-w_c t} - e^{-2w_c t} \end{bmatrix} \tag{15}$$

We get $\exp(\tilde{A}t) \to \mathbf{0}$, $t \to +\infty$ from the Eq.(15). Then defining $\|P\|_{\mathrm{F}} = \sqrt{\sum_{i=1}^{n}\sum_{j}^{n}\left|a_{ij}\right|^2}$ to be the Frobenius norm of matrix $P$ on $K^{n\times n}$, $a_{ij}$ are elements of matrix $P$ and $\|\mathrm{X}\|$ represents the Euclidean norm of a vector X on $K^n$. We know $\|P\|_{\mathrm{F}}$ is compatible with $\|\mathrm{X}\|$, that is $\|P\mathrm{X}\| \leq \|\mathrm{P}\|_{\mathrm{F}}\|\mathrm{X}\|$. Assuming $\left\|\chi\right\| \leq \delta$, we can write:

$$\begin{aligned} \|\tilde{\boldsymbol{\varepsilon}}_i(t)\| &\leq \left\|\exp\left(\tilde{A}t\right)\tilde{\boldsymbol{\varepsilon}}_i(0)\right\| + \left\|\int_0^t \exp\left[\tilde{A}(t-\tau)\right]\frac{\tilde{B}\chi_i}{w_c}d\tau\right\| \\ &\leq \left\|\exp\left(\tilde{A}t\right)\tilde{\boldsymbol{\varepsilon}}_i(0)\right\| + \frac{\left\|\tilde{B}\chi_i\right\|}{w_c}\left\|\int_0^t \exp\left[\tilde{A}(t-\tau)\right]d\tau\right\|_{\mathrm{F}} \\ &\leq \left\|\exp\left(\tilde{A}t\right)\tilde{\boldsymbol{\varepsilon}}_i(0)\right\| + \frac{\delta}{w_c}\left\|-\tilde{A}^{-1}[I-\exp(\tilde{A}t)]\right\|_{\mathrm{F}} \end{aligned} \tag{16}$$

then as $t \to +\infty$ this reduces to

$$\begin{aligned} \|\tilde{\boldsymbol{\varepsilon}}_i(t)\| &\leq \frac{\delta}{w_c}\left\|-\tilde{A}^{-1}\right\|_{\mathrm{F}} \\ &\leq \frac{\sqrt{14}\delta}{2w_c^2} \end{aligned} \tag{17}$$

Next we discuss the neighborhood of $\boldsymbol{\varepsilon}_2$. Since $\|\tilde{\boldsymbol{\varepsilon}}_i\| \leq \frac{\sqrt{14}\delta}{2w_c^2}$, so $|\varepsilon_{2i}| \leq \frac{\sqrt{14}\delta}{2w_c^2}$. The Euclidean norm of $\boldsymbol{\varepsilon}_2$ is given

$$\|\boldsymbol{\varepsilon}_2\| = \sqrt{\varepsilon_{21}^2 + \varepsilon_{22}^2 + \varepsilon_{23}^2} \leq \frac{\sqrt{42}\delta}{2w_c^2} \tag{18}$$

Defining the constant $\sigma_2 = \frac{\sqrt{42}\delta}{2w_c}$, since $\boldsymbol{\varepsilon}_2 = \tilde{\boldsymbol{f}}/w_c$, then as $t \to \infty$ we have that

$$\left\|\tilde{\boldsymbol{f}}\right\| \leq \frac{\sqrt{42}\delta}{2w_c} = \sigma_2 \tag{19}$$

### B. Adaptive Quaternion Feedback control law and Stability Proof

In this subsection we present the design of an adaptive quaternion feedback controller with linear LESO. We define the desired error state of the closed-loop system to be $\boldsymbol{\omega}_{ed} = [0,0,0]^T$ and

$\bar{\boldsymbol{q}}_{ed} = [0, 0, 0, \pm 1]^T$.

The adaptive feedback control law with unknown disturbance estimation is:

$$\boldsymbol{u} = -J_0 \boldsymbol{u}_p - J_0 \hat{\boldsymbol{f}} + (\boldsymbol{\omega}_e + \boldsymbol{C}\boldsymbol{\omega}_d)^{\times} J_0 (\boldsymbol{\omega}_e + \boldsymbol{C}\boldsymbol{\omega}_d) - J_0 \boldsymbol{\omega}_e^{\times} \boldsymbol{C}\boldsymbol{\omega}_d + J_0 \boldsymbol{C}\dot{\boldsymbol{\omega}}_d \tag{20}$$

with

$$\boldsymbol{u}_p = \kappa \boldsymbol{\omega}_e + \lambda q_{e4} \boldsymbol{q}_e \tag{21}$$

and

$$\lambda = \int -k_\lambda \langle \boldsymbol{q}_e, \boldsymbol{q}_e \rangle \, dt + \lambda(0) \tag{22}$$

where, $\kappa > 0$, $\lambda(0) >> k_\lambda > 0$ are scalar constants and $\lambda > 0$.

Then, $\boldsymbol{\omega}_e$ and $\boldsymbol{q}_e$ will converge to a neighborhood of the desired state defined by the upper-bounded error set $B(\boldsymbol{\omega}_e, \boldsymbol{q}_e) \equiv \left\{ (\boldsymbol{\omega}_e, \boldsymbol{q}_e) : \|\boldsymbol{\omega}_e\|^2 + \|\boldsymbol{q}_e\|^4 < \frac{\sigma_2^2}{\kappa k_\lambda} \right\}$, where $\kappa \geq k_\lambda > 0$ and $\sigma_2$ is the upper-bound estimation error of LESO such that $(\lim_{t\to\infty} \boldsymbol{\omega}_e, \lim_{t\to\infty} \boldsymbol{q}_e) \in B(\boldsymbol{\omega}_e, \boldsymbol{q}_e)$.

This can be shown by defining the Lyapunov function $V \geq 0$:

$$V = \frac{1}{2} \langle \boldsymbol{\omega}_e, \boldsymbol{\omega}_e \rangle + \lambda \langle \boldsymbol{q}_e, \boldsymbol{q}_e \rangle \tag{23}$$

with minimum $V = 0$ at $\boldsymbol{\omega}_e = [0, 0, 0]^T$ and $\bar{\boldsymbol{q}}_e = [0, 0, 0, \pm 1]^T$. The time derivative of the Lyapunov function is

$$\dot{V} = \langle \boldsymbol{\omega}_e, \dot{\boldsymbol{\omega}}_e \rangle + \dot{\lambda} \langle \boldsymbol{q}_e, \boldsymbol{q}_e \rangle + 2\lambda \langle \boldsymbol{q}_e, \dot{\boldsymbol{q}}_e \rangle \tag{24}$$

As $\boldsymbol{\omega}_e = \boldsymbol{\omega} - \boldsymbol{C}\boldsymbol{\omega}_d$, recalling Eq.(6) and Eq.(22), the time derivative of this Lyapunov function becomes

$$\dot{V} = \left\langle \boldsymbol{\omega}_e, \dot{\boldsymbol{\omega}} - \dot{\boldsymbol{C}}\boldsymbol{\omega}_d - \boldsymbol{C}\dot{\boldsymbol{\omega}}_d \right\rangle - k_\lambda \langle \boldsymbol{q}_e, \boldsymbol{q}_e \rangle^2 + \lambda \langle \boldsymbol{q}_e, (q_{e4}\boldsymbol{\omega}_e - \boldsymbol{\omega}_e^{\times} \boldsymbol{q}_e) \rangle \tag{25}$$

As $\langle \boldsymbol{q}_e, \boldsymbol{\omega}_e^{\times} \boldsymbol{q}_e \rangle = 0$, substituting $\dot{\boldsymbol{C}} = -\boldsymbol{\omega}_e^{\times} \boldsymbol{C}$ and Eq.(4) into Eq.(25) gives

$$\begin{aligned} \dot{V} = & \left\langle \boldsymbol{\omega}_e, J_0^{-1} (-\boldsymbol{\omega}^{\times} J_0 \boldsymbol{\omega} - \boldsymbol{\omega}^{\times} \Delta J \boldsymbol{\omega} - \Delta J \dot{\boldsymbol{\omega}} + \boldsymbol{u} + \boldsymbol{d}) + \boldsymbol{\omega}_e^{\times} \boldsymbol{C}\boldsymbol{\omega}_d - \boldsymbol{C}\dot{\boldsymbol{\omega}}_d \right\rangle \\ & + \lambda \langle \boldsymbol{q}_e, q_{e4}\boldsymbol{\omega}_e \rangle - k_\lambda \langle \boldsymbol{q}_e, \boldsymbol{q}_e \rangle^2 \end{aligned} \tag{26}$$

Substituting $\boldsymbol{\omega} = \boldsymbol{\omega}_e + \boldsymbol{C}\boldsymbol{\omega}_d$ into Eq.(26) with $\boldsymbol{G}$ and $\boldsymbol{F}$ defined as in Eq.(8), the Eq.(26) simplifies to

$$\begin{aligned}\dot{V} &= \left\langle \boldsymbol{\omega}_e, \boldsymbol{F} + \boldsymbol{G} + J_0^{-1}\boldsymbol{u} + J_0^{-1}\boldsymbol{d} \right\rangle + \lambda \left\langle \boldsymbol{\omega}_e, q_{e4}\boldsymbol{q}_e \right\rangle - k_\lambda \langle \boldsymbol{q}_e, \boldsymbol{q}_e \rangle^2 \\ &= \left\langle \boldsymbol{\omega}_e, \boldsymbol{F} + \boldsymbol{G} + J_0^{-1}\boldsymbol{u} + J_0^{-1}\boldsymbol{d} + \lambda q_{e4}\boldsymbol{q}_e \right\rangle - k_\lambda \left\langle \boldsymbol{q}_e, \boldsymbol{q}_e \right\rangle^2\end{aligned} \tag{27}$$

Substituting the control law Eq.(20) into Eq.(27) gives

$$\dot{V} = \left\langle \boldsymbol{\omega}_e, -\kappa\boldsymbol{\omega}_e + \boldsymbol{f} - \hat{\boldsymbol{f}} \right\rangle - k_\lambda \left\langle \boldsymbol{q}_e, \boldsymbol{q}_e \right\rangle^2 \tag{28}$$

Since $\tilde{\boldsymbol{f}} = \boldsymbol{f} - \hat{\boldsymbol{f}}$ and $\|\tilde{\boldsymbol{f}}\| \leq \sigma_2$ when $t \to \infty$, then Eq.(28) can be written as

$$\begin{aligned}\lim_{t\to\infty} \dot{V} &= \left\langle \boldsymbol{\omega}_e, -\kappa\boldsymbol{\omega}_e + \tilde{\boldsymbol{f}} \right\rangle - k_\lambda \left\langle \boldsymbol{q}_e, \boldsymbol{q}_e \right\rangle^2 \\ &= -\kappa \left\langle \boldsymbol{\omega}_e, \boldsymbol{\omega}_e \right\rangle - k_\lambda \left\langle \boldsymbol{q}_e, \boldsymbol{q}_e \right\rangle^2 + \left\langle \boldsymbol{\omega}_e, \tilde{\boldsymbol{f}} \right\rangle\end{aligned} \tag{29}$$

using the Cauchy-Schwartz inequality we have

$$\left| \left\langle \boldsymbol{\omega}_e, \tilde{\boldsymbol{f}} \right\rangle \right| \leq \left\| \tilde{\boldsymbol{f}} \right\| \|\boldsymbol{\omega}_e\| \tag{30}$$

so a sufficient condition for $\lim_{t\to\infty} \dot{V} \leq 0$ can be written as

$$\kappa \left\langle \boldsymbol{\omega}_e, \boldsymbol{\omega}_e \right\rangle + k_\lambda \langle \boldsymbol{q}_e, \boldsymbol{q}_e \rangle^2 \geq \left\| \tilde{\boldsymbol{f}} \right\| \|\boldsymbol{\omega}_e\| \tag{31}$$

and as $\lim_{t\to\infty, k_\lambda \to 0} \dot{V} \leq 0$ means that $\kappa \|\boldsymbol{\omega}_e\| \geq \left\| \tilde{\boldsymbol{f}} \right\|$ then $\|\boldsymbol{\omega}_e\| > \sigma_2/\kappa$ is a sufficient condition for $\lim_{t\to\infty, k_\lambda \to 0} \dot{V} \leq 0$ and the fact that $\lim_{t\to\infty} \dot{V} \leq \lim_{t\to\infty, k_\lambda \to 0} \dot{V} \leq 0$ then a sufficient condition for $\lim_{t\to\infty} \dot{V} \leq 0$ is

$$\kappa \left\langle \boldsymbol{\omega}_e, \boldsymbol{\omega}_e \right\rangle + k_\lambda \langle \boldsymbol{q}_e, \boldsymbol{q}_e \rangle^2 \geq \frac{\sigma_2^2}{\kappa} \tag{32}$$

Conversely if $\kappa \left\langle \boldsymbol{\omega}_e, \boldsymbol{\omega}_e \right\rangle + k_\lambda \langle \boldsymbol{q}_e, \boldsymbol{q}_e \rangle^2 \leq \frac{\sigma_2^2}{\kappa}$ then the tracking errors are within a small, bounded neighborhood of the desired state. Given the assumption $\kappa \geq k_\lambda > 0$, then $\frac{\kappa}{k_\lambda} \langle \boldsymbol{\omega}_e, \boldsymbol{\omega}_e \rangle + \langle \boldsymbol{q}_e, \boldsymbol{q}_e \rangle^2 \leq$

$\frac{\langle \omega_e, \tilde{f} \rangle}{k_\lambda} \leq \frac{\|\tilde{f}\|}{k_\lambda}\|\omega_e\| \leq \frac{\sigma_2^2}{\kappa k_\lambda}$, so $\|\omega_e\|^2 + \|q_e\|^4 \leq \frac{\kappa}{k_\lambda}\langle \omega_e, \omega_e \rangle + \langle q_e, q_e \rangle^2 \leq \frac{\sigma_2^2}{\kappa k_\lambda}$. Therefore

$$\|\omega_e\|^2 + \|q_e\|^4 \leq \frac{\sigma_2^2}{\kappa k_\lambda} \tag{33}$$

provides an upper-bound for the tracking error. It is clear from Eq.(33) that increasing $\kappa$ and $k_\lambda$, for a given upper-bound $\sigma_2$ of the error of the estimator, will decrease the size of the error set $B(\omega_e, q_e)$. Although theoretically the set $B(\omega_e, q_e)$ would converge to a zero set if $\kappa, k_\lambda \to \infty$, it is impossible due to the physical limits of the actuator in practice. Note that it could be possible to use a different adaptive gains with the extended state observer and compare this in terms of performance. However, the adaptive gain Eq.(22) is central to the proof that the region of convergence is controllable i.e. the derivative of the Lyapunov function would otherwise not include the quaternion error and thus only an upper-bound on the angular velocity error would be controllable.

## IV. Simulation and Analysis

In this section, we implement the control law (20) in simulation on a representative 3U CubeSat [25] to perform a slew motion in the presence of parameter, disturbance uncertainty and RW friction with:

$$J_0 = diag\,[0.0109, 0.0506, 0.0506] \quad kg \cdot m^2 \tag{34}$$

In each case the proposed controller is compared to a traditional flight tested quaternion control method.

### A. Slew motions in the presence of unknown parameter uncertainty and disturbances

The error of the inertia matrix is taken to be:

$$\Delta J = \begin{bmatrix} 0.005 & 0.001 & 0.0015 \\ 0.001 & 0.025 & 0.002 \\ 0.0015 & 0.002 & 0.025 \end{bmatrix} \quad kg \cdot m^2 \tag{35}$$

and a sinusoidal disturbance torque is assumed:

$$\boldsymbol{d} = \begin{bmatrix} \sin 0.01\pi t \\ \sin 0.02\pi t \\ \sin 0.04\pi t \end{bmatrix} \times 10^{-4} N \cdot m \tag{36}$$

A simple PID quaternion feedback controller is used for comparison which is stated as:

$$u_{pid} = k_p \boldsymbol{q}_e + k_i \int \boldsymbol{q}_e dt + k_d \boldsymbol{\omega}_e \tag{37}$$

where, $k_p \leq 0$, $k_i \leq 0$, $k_d \leq 0$ are the proportional, integral and differential gains.

Although all the simulations are undertaken using quaternions we plot the corresponding Euler angles over time to demonstrate clearly the pointing accuracy in an intuitive coordinate system. Let the desired quaternion $\bar{\boldsymbol{q}}_d\left(t_f\right) = [1, 0, 0, 0]^T$, correspond to the Euler angles (pitch, roll, yaw) are $(0, 0, 0)\, deg$ and $\boldsymbol{\omega}_d = [0, 0, 0]^T\, rad/s$, the initial angular velocity $\boldsymbol{\omega} = [0, 0, 0]^T\, rad/s$ and the initial quaternion value $\bar{\boldsymbol{q}}\,(0) = [0.9537, 0.1736, -0.1736, 0.1736]^T$, which corresponds to the Euler angles $(-17.1223, 23.0493, 17.1223)\, deg$. The gain $\kappa = 50$, $k_\lambda = 0.1$ and $\lambda\,(0) = 10$, the linear LESO parameter $\beta_1 = 30, \beta_2 = 200$ $(w_c = 10)$ and the maximum control torque corresponding to a typical maximum torque of a 3U CubeSat reaction wheel is $u_{max} \leq 10^{-3} N \cdot m$. The value of the PID control gains are manually tuned to obtain good tracking performance, for our chosen example, as $k_p = -0.6011, k_i = 0, k_d = -1.7808$.

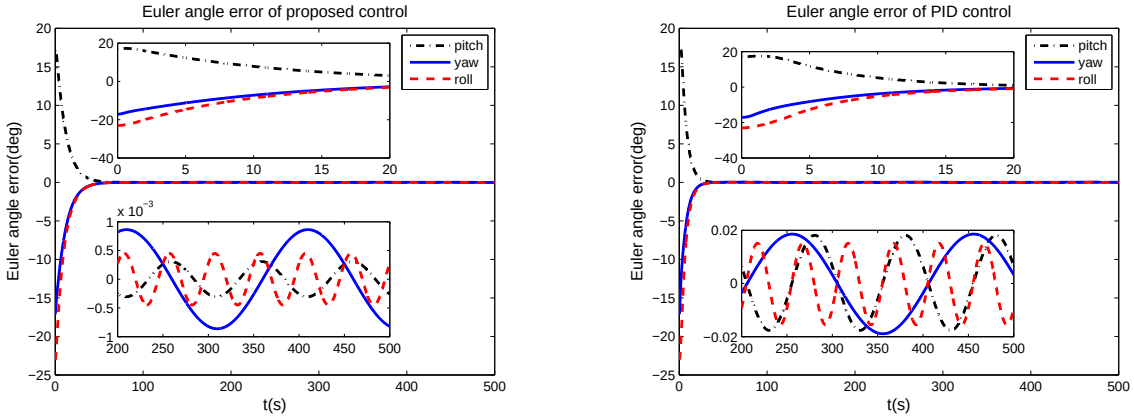


**Figure 1. Euler angle tracking error**

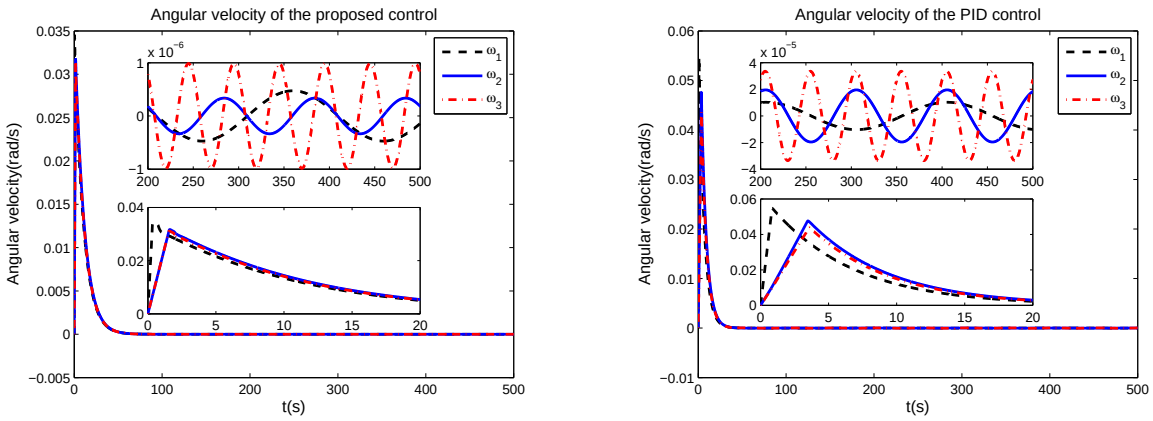


**Figure 2. Angular velocity**

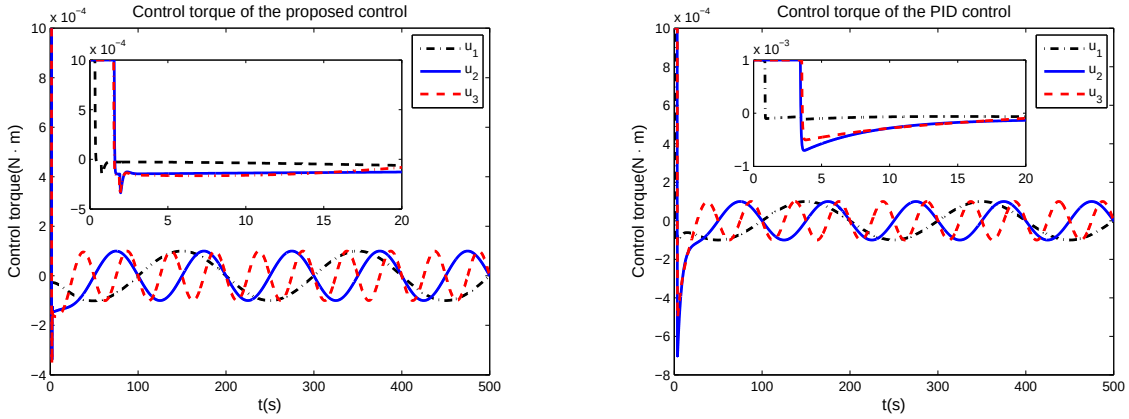


**Figure 3. Control torque**

In Fig.1 it can be seen that the Euler angle tracking error of the proposed control has a stabilization error typically less than $1\times10^{-3}deg$. The error of the PID control, in contrast, is about 0.02 *deg* which is 50 times greater than the proposed control. In practise, a star sensor would also be used for precision pointing and has an error of less than 100 *arcsec* [26] (100 *arcsec* = 0.028 *deg*). Hence, the proposed control could provide a significant improvement to a conventional PID control in terms of pointing accuracy. Fig.2 illustrates the angular velocity of the proposed control and PID control. The corresponding control torque is shown in Fig.3. Fig.4 indicates the disturbance estimation performance of LESO where $[E_1, E_2, E_3]^T = J_0\tilde{\boldsymbol{f}}$. Fig.5 illustrates the adaptive gain $\lambda$ during the maneuver. In this example, it can be seen from the figures that the proposed controller is effective at dealing with the disturbances and shows a significant improvement when compared to the PID controller, for the chosen example, in pointing capability in the presence of uncertainty

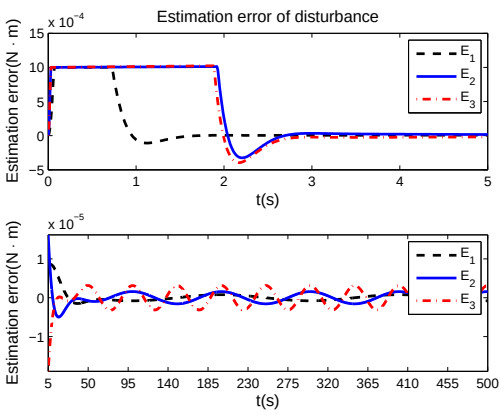


**Figure 4. Estimation error of the disturbance via LESO**

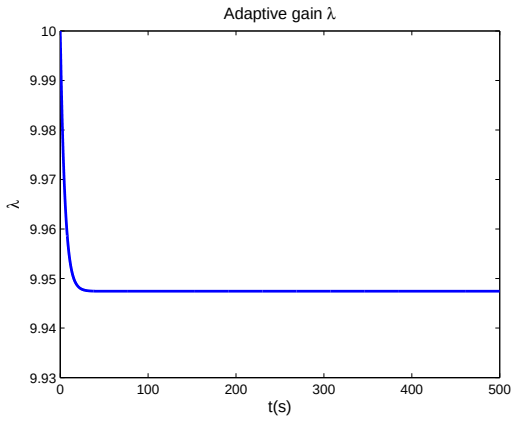


**Figure 5. Adaptive gain**

**Table 1. Comparison results proposed control without sensor error**

| | $0.01\boldsymbol{d}$ | $0.1\boldsymbol{d}$ | $\boldsymbol{d}$ |
|---|---|---|---|
| $\Delta J$ | $7.3918 \times 10^{-6}$ | $7.3951 \times 10^{-5}$ | $7.3954 \times 10^{-4}$ |
| $2\Delta J$ | $7.3936 \times 10^{-6}$ | $7.3969 \times 10^{-5}$ | $7.3972 \times 10^{-4}$ |
| $3\Delta J$ | $7.3953 \times 10^{-6}$ | $7.3987 \times 10^{-5}$ | $7.3990 \times 10^{-4}$ |

without significantly altering the required torque.

The components of Table 1 show values for the average Euclidean norm $\|\boldsymbol{q}_e\|$ over the period $t \in [200, 500]$ secs. Table 1 demonstrates that a significant increase in the uncertainty in the inertia matrix does not significantly effect the pointing accuracy of the proposed control. Also decreasing the disturbance to magnitudes of order more typical of a 3U CubeSat in LEO shows that even higher pointing accuracy can be obtained. In this part, the upper-bound on the size of the convergence neighborhood from 200 to 500s is $B(\boldsymbol{\omega}_e, \boldsymbol{q}_e) \equiv \left\{(\boldsymbol{\omega}_e, \boldsymbol{q}_e) : \|\boldsymbol{\omega}_e\|^2 + \|\boldsymbol{q}_e\|^4 < 1.3854 \times 10^{-8}\right\}$ using Eq.(33). The tracking errors in the simulation can be observed to remain within this neighborhood.

## B. A friction compensation control

In this example we demonstrate the efficiency of the proposed control as a friction compensation control. Moreover, it is shown that the proposed control can significantly improve the pointing accuracy of a nano-spacecraft in the presence of significant RW friction. The friction torque ap-

plied to the RWs are given by the equation [22]:

$$\boldsymbol{d}_f = \beta_d \boldsymbol{\Omega} + \left[\beta_k + \beta_s / \left(1 + \boldsymbol{\Omega}^2 / \boldsymbol{\Omega}_s^2\right)\right] sgn\left(\boldsymbol{\Omega}\right) \tag{38}$$

where $\boldsymbol{d}_f = \left[d_{f1}, d_{f2}, d_{f3}\right]^T$ is the friction torque, $\boldsymbol{\Omega} = [\Omega_1, \Omega_2, \Omega_3]^T$ is the angular velocity of the wheels, $\beta_d$ is unknown viscous friction coefficient, $\beta_k$ denotes the Coulomb friction torque, $\beta_s$ is unknown Stribeck friction torque, $\Omega_s$ denotes characteristic speed of Stribeck friction and $sgn(\cdot)$ is standard sign function. Note that the disturbance (38) is only piecewise continuously differentiable as if an angular velocity of the reaction wheel crosses zero there is a discontinuity in the derivative of the disturbance. In practise this will cause an error in the LESO at this point and a short transient before it converges to the correct estimate. In this case the attitude dynamics are

$$J\dot{\boldsymbol{\omega}} = -\boldsymbol{\omega} \times (J\boldsymbol{\omega} + \boldsymbol{h}) + \boldsymbol{u} + \boldsymbol{d}_f \tag{39}$$

where $\boldsymbol{h} = J_\Omega \boldsymbol{\Omega}$ is the angular momentum of the RW and the $J_\Omega$ denotes inertia matrix of the wheels. In this part, the uncertainty of the inertia matrix is ignored ($\Delta J = \mathbf{0}$). The corresponding linear LESO is given as

$$\begin{aligned} \dot{\hat{\boldsymbol{\omega}}} &= \hat{\boldsymbol{d}}_f + \beta_1 I_3 \left(\boldsymbol{\omega} - \hat{\boldsymbol{\omega}}\right) - J^{-1}\boldsymbol{\omega} \times (J\boldsymbol{\omega} + \boldsymbol{h}) + J^{-1}\boldsymbol{u} \\ \dot{\hat{\boldsymbol{d}}}_f &= \beta_2 I_3 \left(\boldsymbol{\omega} - \hat{\boldsymbol{\omega}}\right) \end{aligned} \tag{40}$$

where $\hat{\boldsymbol{\omega}}$ is the estimated value of $\boldsymbol{\omega}$ and $\hat{\boldsymbol{d}}_f$ is the estimated value of $\boldsymbol{d}_f$.

The inertia matrix of the wheels is $J_\Omega = diag\left[1.5, 1.5, 1.5\right] \times 10^{-4} kg \cdot m^2$, $\beta_d = 1.18 \times 10^{-6} Nms/rad$, $\beta_k = 2 \times 10^{-5} Nm$, $\beta_s = 1.5 \times 10^{-5} Nm$ and $\Omega_s = 2.5 rad/s$. The maximum allowable control torque of a typical nano-RW is set to $u_{max} \leq 10^{-3} N \cdot m$ and the maximum momentum of each RW is $h_{max} \leq 0.015 N \cdot m \cdot s$. The corresponding friction torque curve against angular velocity for these RWs under the above conditions is shown in Fig.6.

The proposed control gains, LESO parameters and PID control gains are the same as subsection A of section IV. The initial quaternion $\bar{\boldsymbol{q}}(0) = [0.3, -0.2, -0.3, 0.8832]^T$, corresponding Euler angles (pitch, roll, yaw) are $(-35.7768, 24.1987, 134.5613)\, deg$ and angular velocity

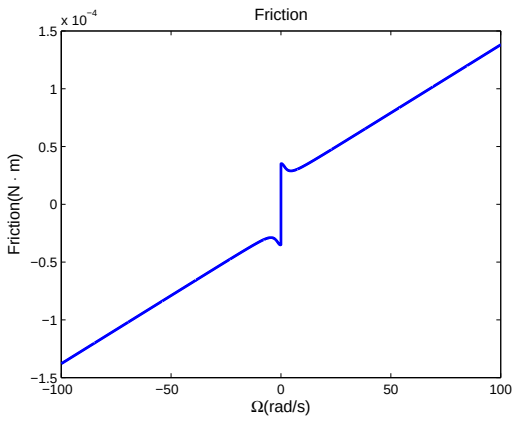


**Figure 6. Friction torque curve against angular velocity of RWs**

$\boldsymbol{\omega} = [0,0,0]^T\ rad/s$, the desired quaternion $\bar{\boldsymbol{q}}_d = [0.5,-0.5,-0.5,0.5]^T$, corresponding Euler angles are $(-90,0,90)\,deg$ and $\boldsymbol{\omega}_d = [0,0,0]^T\ rad/s$.

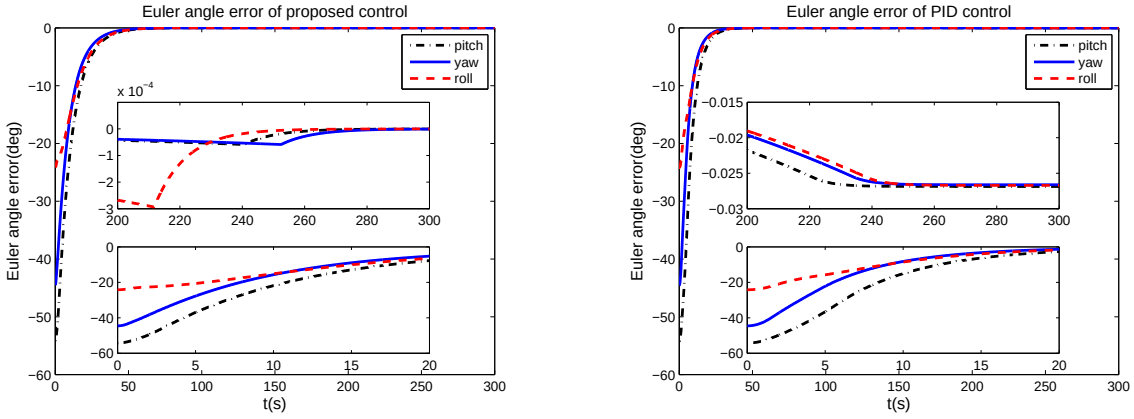


**Figure 7. Euler angle tracking error with friction**

There is a significant increase in pointing accuracy when using the control proposed in this paper compared with a PID controller as can be seen in the steady-state behavior of Fig.7. It can be seen that the Euler angle tracking error of the proposed control has an error less than $3\times10^{-4}deg$ which reflects a high pointing accuracy for a nano-spacecraft. The error of the PID control is about 0.027 $deg$ which is 90 times greater than the proposed control. The comparison of angular velocity and control torque are shown in Fig.8 and Fig.9 respectively. The comparison demonstrates that the proposed control is far more robust than conventional control. Fig.10 and Fig.11 illustrate the friction torque of the RWs. The estimation of the friction is given in Fig.12 and demonstrates that the LESO has a very high accuracy where $[\xi_1,\xi_2,\xi_3]^T = J_0(\boldsymbol{d}_f - \hat{\boldsymbol{d}}_f)$. Since friction can be estimated

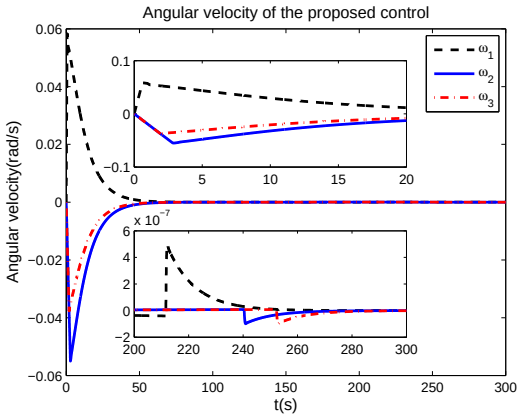


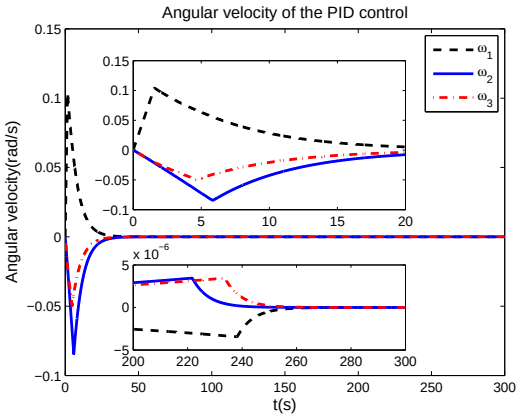


**Figure 8. Angular velocity with friction**

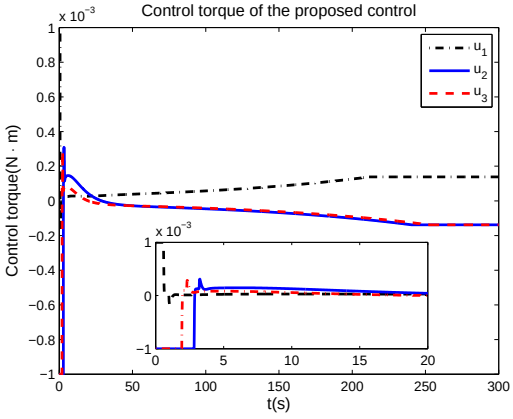


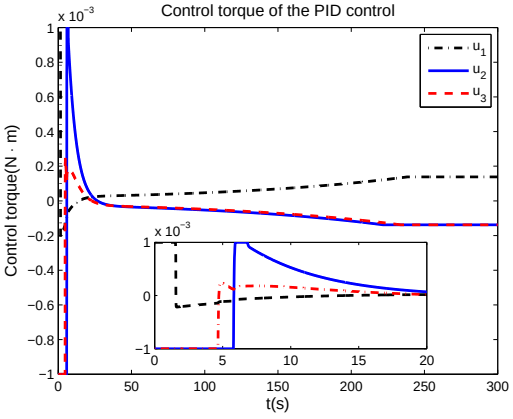


**Figure 9. Control torque with friction**

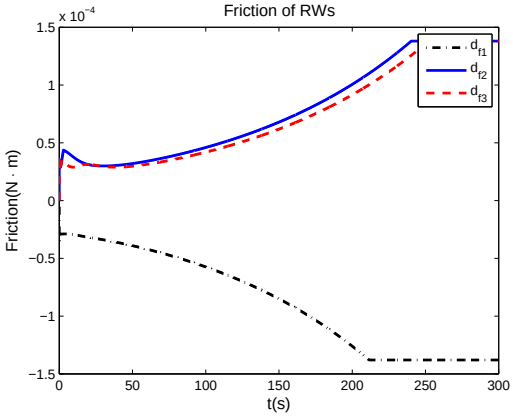


**Figure 10. Friction torque of proposed control**

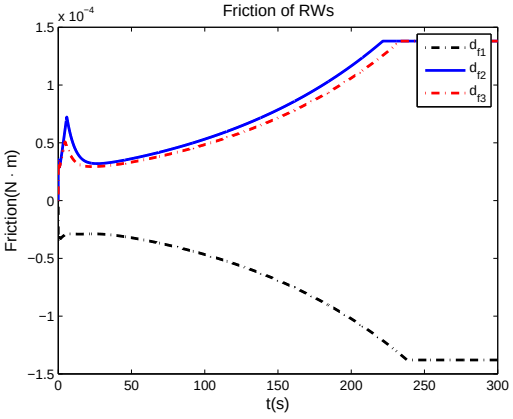


**Figure 11. Friction torque of PID**

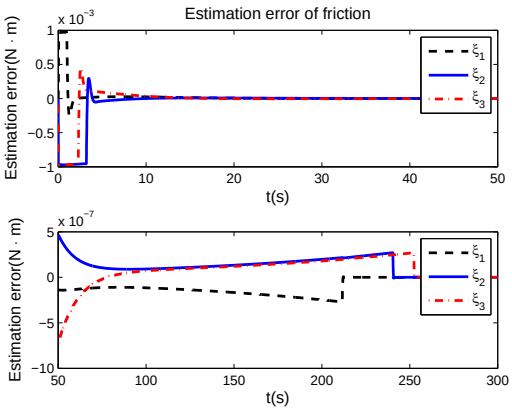


**Figure 12. Estimation error of the friction via LESO**

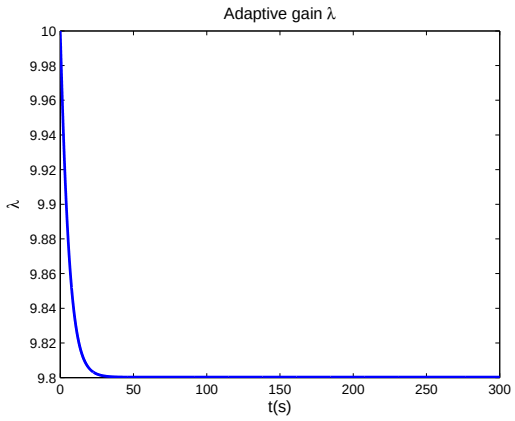


**Figure 13. Adaptive gain**

accurately with LESO there is no benefit to using a nonlinear state observer which would increase computational expense and tuning complexity. Fig.13 demonstrates the adaptive gain $\lambda$. In this part, the size of the convergence neighborhood from 200 to 300s can be observed to remain in the upper-bounded set $B(\boldsymbol{\omega}_e, \boldsymbol{q}_e) \equiv \left\{(\boldsymbol{\omega}_e, \boldsymbol{q}_e) : \|\boldsymbol{\omega}_e\|^2 + \|\boldsymbol{q}_e\|^4 < 1.5447 \times 10^{-8}\right\}$ given by Eq.(33).

## V. Conclusion

An adaptive quaternion based feedback control with linear disturbance rejection has been presented and proved to track a desired motion within a small bounded neighborhood, in the presence uncertainties in the moments of inertia and external disturbance torques. Provided that the controller satisfies the stated gain constraints the convergence to a small neighborhood of the reference trajectory is guaranteed even in the presence of a disturbance estimation error. An upper limit to this small bounded region was computed analytically and is shown to be controllable by varying the gains. However, although controllable, the upper limit of the tracking error is constrained by the gain constraint and the physical constraints of the actuators. Simulations have demonstrated that this control law can effectively track a prescribed attitude motion in the presence of uncertainty in the moments of inertia, unknown environmental disturbances and reaction wheel friction. There is a significant improvement in pointing accuracy, for our chosen example, in the presence of these uncertainties when compared to a conventional controller and used alongside a star sensor could provide high pointing accuracy in practical applications. The analysis shows that the adaptive parameter reduces the neighborhood of the tracking error and that this neighborhood is reducible by

appropriate tuning of the gain parameters. Furthermore, this control does not suffer the problem of chattering that is apparent in sliding mode controllers with disturbance rejection control. Future work will include using adaptive uncertainty rejection control in new application areas such as, in spacecraft docking and six-degree of freedom relative motion problems. Furthermore, the presence of a noisy disturbance will require the amalgamation of our control technique with a filter in order to satisfy the assumptions of the extended state observer.

## References


[1] Li, Z. X., and Wang, B. L., "Robust Attitude Tracking Control of Spacecraft in the Presence of Disturbances," *Journal of Guidance, Control, and Dynamics*, Vol. 30, No. 4, 2007, pp. 1156-1159. doi: 10.2514/1.26230

[2] Luo, W., Chu, Y., and Ling, K., "H-Infinity Inverse Optimal Attitude-Tracking Control of Rigid Spacecraft," *Journal of Guidance, Control, and Dynamics*, Vol. 28, No. 3, 2005, pp. 481-494. doi: 10.2514/1.6471

[3] Thakur, D., Srikant, S. and Akella, M.R., "Adaptive Attitude-Tracking Control of Spacecraft with Uncertain Time-Varying Inertia Parameters," *Journal of Guidance, Control, and Dynamics*, Vol. 38, No. 1, 2015, pp. 41-52. doi: 10.2514/1.G000457

[4] Yoon, H. and Tsiotras, P., "Spacecraft Adaptive Attitude and Power Tracking with Variable Speed Control Moment Gyroscopes," *Journal of Guidance, Control, and Dynamics*, Vol. 25, No. 6, 2002, pp. 1081-1090. doi: 10.2514/2.4987

[5] Costic, B. T., Dawson, D. M.,de Queiroz et, M. S., and Kapila, V., "Quaternion-Based Adaptive Attitude Tracking Controller Without Velocity Measurements," *Journal of Guidance, Control, and Dynamics*, Vol. 24, No. 6, 2001, pp. 1214-1222. doi: 10.2514/2.4837

[6] Wallsgrove, R. J., and Akella, M. R., "Globally Stabilizing Saturated Attitude Control in the Presence of Bounded Unknown Disturbances," *Journal of Guidance, Control, and Dynamics*, Vol. 28, No. 5, 2005, pp. 957-963. doi: 10.2514/1.9980

[7] Y. Han, Biggs, J. D and N. G. Cui., "Adaptive Fault-Tolerant Control of Spacecraft Attitude Dynamics with Actuator Failures," *Journal of Guidance, Control, and Dynamics*, Vol. 38, No. 10, 2015, pp. 2033-2042. doi: 10.2514/1.G000921

[8] Zhu,Z. Xia,Y.Q. and Fu, M.Y., "Adaptive Sliding Mode Control for Attitude Stabilization With Actuator Saturation," *IEEE Transactions On Industrial Electronics*, Vol. 58, No. 10, 2011, pp. 4898-4907. doi: 10.1109/TIE.2011.2107719

[9] Lo,S.C. and Chen, Y.P., "Smooth sliding-mode control for spacecraft attitude tracking maneuvers," *Journal of Guidance, Control, and Dynamics*, Vol. 18, No. 6, 1995, pp. 1345-1349. doi: 10.2514/3.21551

[10] Pukdeboon, C., Zinober, A. S. I. and Thein, M.-W. L. "Quasi-continuous higher-order sliding mode controllers for spacecraft attitude tracking maneuvers," *IEEE Transactions On Industrial Electronics*, Vol. 57, No. 4, 2010, pp. 1436-1444. doi: 10.1109/TIE.2009.2030215

[11] W. Luo, Y.-C. Chu, and K.-V. Ling, "Inverse optimal adaptive control for attitude tracking of spacecraft," *IEEE Transactions on Automatic Control*, Vol. 50, No. 11, 2005, pp. 1639-1654. doi: 10.1109/TAC.2005.858694

[12] C.-D. Yang and C.-C. Kung, "Nonlinear flight control of general six-degree-of-freedom motions," *Journal of Guidance, Control, and Dynamics*, Vol. 23, No. 2, 2000, pp. 278-288. doi: 10.2514/2.4520

[13] Z. Chen and J. Huang, "Attitude tracking and disturbance rejection of rigid spacecraft by adaptive control," *IEEE Transactions on Automatic Control*, Vol. 54, No. 3, 2009, pp. 600-605. doi: 10.1109/TAC.2008.2008350

[14] J. Q. Han, "From PID to active disturbance rejection control," *IEEE Transactions on Industrial Electronics*, Vol. 56, No. 3, 2009, pp. 900-906. doi: 10.1109/TIE.2008.2011621

[15] Z. Gao, S. Hu and F. Jiang, "A novel motion control design approach based on active disturbance rejection," *In Proceedings of the 40th IEEE Conference on Decision and Control*, IEEE, Orlando, USA, 2001, pp. 4898-4907. doi: 10.1109/.2001.980980

[16] S. Li, X. Yang, and D. Yang, "Active disturbance rejection control for high pointing accuracy and rotation speed," *Automatica*, vol. 45, No. 8, 2009, pp. 1854-1860. doi: 10.1016/j.automatica.2009.03.029

[17] Xia,Y.Q., Zhu,Z., Fu, M.Y. and Wang, S., "Attitude Tracking of Rigid Spacecraft With Bounded Disturbances," *IEEE Transactions On Industrial Electronics*, Vol. 58, No. 2, 2011, pp. 647-659. doi: 10.1109/TIE.2010.2046611

[18] Zhong, C.X., Guo, Y. and Wang, L., "Fuzzy Active Disturbance Rejection Attitude Control of Spacecraft with Unknown Disturbance and Parametric Uncertainty," *International Journal of Control and Automation*, Vol. 8, No. 8, 2015, pp. 233-242. doi: 10.14257/ijca.2015.8.8.24

[19] Bai, Y. Biggs, J.D., Wang, X, Ciu, N., "A singular adaptive attitude control with active disturbance rejection," *European Journal of Control*, Vol. 35, 2017, pp. 50-56. doi: 10.1016/j.ejcon.2017.01.002

[20] Q. Zheng, L. Gao, Z. Q. Gao, "On stability analysis of active disturbance rejection control for nonlinear time-varying plants with unknown dynamics," *In Proceedings of the 46th IEEE Conference on Decision and Control*, IEEE. New Orleans, USA, 2007, pp. 3501-3506. doi: 10.1109/CDC.2007.4434676

[21] B. Z. Guo and Z. L. Zhao, "On the convergence of an extended state observer for nonlinear systems with uncertainty," *Systems & Control Letters*, Vol. 60, No. 6, 2011, pp. 420-430. doi: 10.1016/j.sysconle.2011.03.008

[22] X. B. Cao, B. L. Wu, "Indirect adaptive control for attitude tracking of spacecraft with unknown reaction wheel friction," *Aerospace Science and Technology*, Vol. 47, 2015, pp. 493-500. doi: 10.1016/j.ast.2015.10.017

[23] M. J Sidi, "Spacecraft Dynamics and Control," Cambridge, U.K: Cambridge University Press, 1997.

[24] Wie, B., "Space Vehicle Dynamics and Control," 2nd ed., AIAA, Reston, VA, 2008, pp. 340.

[25] Maclean, C., Pagnozzi, D. and Biggs, J. D., "Planning Natural Repointing Manoeuvres for Nano-Spacecraft," *IEEE Transactions on Aerospace and Electronic Systems*, Vol. 50, No. 3, 2014, pp. 2129-2145. doi: 1109/TAES.2014.130417

[26] R. C. Olsen, "Remote Sensing from Air and Space," Bellingham: The International Society for Optical Engineering, 2007.